

## New Isotopes and Proton Emitters—Crossing the Drip Line in the Vicinity of $^{100}\text{Sn}$

I. Čeliković,<sup>1,2,\*</sup> M. Lewitowicz,<sup>1</sup> R. Gernhäuser,<sup>3</sup> R. Krücken,<sup>4,5</sup> S. Nishimura,<sup>6</sup> H. Sakurai,<sup>7</sup> D.S. Ahn,<sup>6</sup> H. Baba,<sup>6</sup> B. Blank,<sup>8</sup> A. Blazhev,<sup>9</sup> P. Boutachkov,<sup>10</sup> F. Browne,<sup>6,11</sup> G. de France,<sup>1</sup> P. Doornenbal,<sup>6</sup> T. Faestermann,<sup>3,12</sup> Y. Fang,<sup>13</sup> N. Fukuda,<sup>6</sup> J. Giovinazzo,<sup>8</sup> N. Goel,<sup>10</sup> M. Górska,<sup>10</sup> S. Ilieva,<sup>14</sup> N. Inabe,<sup>6</sup> T. Isobe,<sup>6</sup> A. Jungclaus,<sup>15</sup> D. Kameda,<sup>6</sup> Y.-K. Kim,<sup>16,17</sup> Y. K. Kwon,<sup>16</sup> I. Kojouharov,<sup>10</sup> T. Kubo,<sup>6</sup> N. Kurz,<sup>10</sup> G. Lorusso,<sup>6</sup> D. Lubos,<sup>3,6,12</sup> K. Moschner,<sup>9</sup> D. Murai,<sup>6</sup> I. Nishizuka,<sup>18</sup> J. Park,<sup>4,5</sup> Z. Patel,<sup>6,19</sup> M. Rajabali,<sup>4</sup> S. Rice,<sup>6,19</sup> H. Schaffner,<sup>10</sup> Y. Shimizu,<sup>6</sup> L. Sinclair,<sup>6,20</sup> P.-A. Söderström,<sup>6</sup> K. Steiger,<sup>3</sup> T. Sumikama,<sup>18</sup> H. Suzuki,<sup>6</sup> H. Takeda,<sup>6</sup> Z. Wang,<sup>4</sup> H. Watanabe,<sup>21</sup> J. Wu,<sup>6,22</sup> and Z. Xu<sup>7</sup>

<sup>1</sup>Grand Accélérateur National d'Ions Lourds (GANIL), CEA/DRF-CNRS/IN2P3, Boulevard H. Becquerel, 14076 Caen, France

<sup>2</sup>“Vinča” Institute of Nuclear Sciences, University of Belgrade, 11000 Belgrade, Serbia

<sup>3</sup>Physik Department E12, Technische Universität München, D-85748 Garching, Germany

<sup>4</sup>TRIUMF, Vancouver, British Columbia V6T 2A3, Canada

<sup>5</sup>Department of Physics and Astronomy, University of British Columbia, Vancouver, British Columbia V6T 1Z1, Canada

<sup>6</sup>RIKEN Nishina Center, 2-1 Hirosawa, Wako, Saitama 351-0198, Japan

<sup>7</sup>University of Tokyo, 7-3-1 Hongo Bunkyo, Tokyo 113-0033, Japan

<sup>8</sup>CEN Bordeaux-Gradignan Le Haut-Vigneau, F-33175 Gradignan Cedex, France

<sup>9</sup>Institute of Nuclear Physics, University of Cologne, D-50937 Cologne, Germany

<sup>10</sup>GSI Helmholtzzentrum für Schwerionenforschung GmbH, D-64291 Darmstadt, Germany

<sup>11</sup>School of Computing, Engineering and Mathematics, University of Brighton, Brighton BN2 4GJ, United Kingdom

<sup>12</sup>Excellence Cluster Universe, Technische Universität München, D-85748 Garching, Germany

<sup>13</sup>Osaka University, Machikaneyama-machi 1-1, Osaka 560-0043 Toyonaka, Japan

<sup>14</sup>Technische Universität Darmstadt, D-64289 Darmstadt, Germany

<sup>15</sup>Instituto de Estructura de la Materia, IEM-CSIC, E-28006 Madrid, Spain

<sup>16</sup>Rare Isotope Science Project, Institute for Basic Science, Daejeon 305-811, Republic of Korea

<sup>17</sup>Department of Nuclear Engineering, Hanyang University, Seoul 133-791, Republic of Korea

<sup>18</sup>Department of Physics, Faculty of Science, Tohoku University, Sendai 980-0845, Japan

<sup>19</sup>Department of Physics, University of Surrey, Guildford GU2 7XH, United Kingdom

<sup>20</sup>University of York, York YO10 5DD, United Kingdom

<sup>21</sup>Beihang University, Beijing 100191, China

<sup>22</sup>Department of Physics, Peking University, Beijing 100871, China

(Received 19 January 2016; revised manuscript received 7 March 2016; published 20 April 2016)

Several new isotopes,  $^{96}\text{In}$ ,  $^{94}\text{Cd}$ ,  $^{92}\text{Ag}$ , and  $^{90}\text{Pd}$ , have been identified at the RIKEN Nishina Center. The study of proton drip-line nuclei in the vicinity of  $^{100}\text{Sn}$  led to the discovery of new proton emitters  $^{93}\text{Ag}$  and  $^{89}\text{Rh}$  with half-lives in the submicrosecond range. The systematics of the half-lives of odd- $Z$  nuclei with  $T_z = -1/2$  toward  $^{99}\text{Sn}$  shows a stabilizing effect of the  $Z = 50$  shell closure. Production cross sections for nuclei in the vicinity of  $^{100}\text{Sn}$  measured at different energies and target thicknesses were compared to the cross sections calculated by EPAX taking into account contributions of secondary reactions in the primary target.

DOI: 10.1103/PhysRevLett.116.162501

For atomic nuclei one basic property is the number of nucleons the strong interaction can confine to form a bound system. The borders between bound and unbound systems, the drip lines, are determined by the change in sign of the single-nucleon separation energies ( $S_n$  and  $S_p$  for neutron and proton, respectively) determined from the binding energy differences between a nucleus and its immediate lighter isotope (for  $S_n$ ) or isotone (for  $S_p$ ). At the proton drip line, the potential barrier confines the protons and hampers particle emission. However, when the penetration probability is large enough, proton, two-proton, and  $\alpha$  radioactivity can compete with  $\beta$  decay. Observing direct proton emission allows one to study nuclear structure even beyond the proton drip line.

Because of the Coulomb repulsion, the proton drip line lies closer to the valley of  $\beta$  stability as compared to the neutron drip line, and for almost all elements up to protactinium ( $Z = 91$ ), the proton drip line has been reached for odd- $Z$  elements [1]. The first evidence of proton emission was obtained from the decay studies of a high-spin isomer in  $^{53}\text{Co}$  [2], while the first ground-state proton emission was observed in  $^{151}\text{La}$  and  $^{147}\text{Tm}$  more than 30 years ago [3,4]. Since then, a considerable number of proton emitters beyond the drip line have been observed [5,6].

The detection of proton radioactivity can yield simple observables such as the decay energy and the half-life, which can be used to extract information on the nuclear

wave function and can serve to constrain nuclear mass models. Of particular interest is proton radioactivity from nuclei with  $Z < 50$  since they serve as an important input to calculate the path of the  $rp$  process [7].

With the impressive progress in the in-flight production of nuclei with extreme neutron-to-proton ratios as well as the construction of a new generation of fragment separators in RIKEN, GSI, or MSU, new regions of the nuclear landscape become accessible, and, in particular, the region of the doubly magic  $^{100}\text{Sn}$  isotope [8]. In this Letter we report on the discovery of new isotopes at the proton drip line and on evidence for new proton emitters.

The measurements were performed at the RIKEN Nishina Center with the BigRIPS separator [9]. The quest for new isotopes at the limits of nuclear binding is one of the major research lines in nuclear physics and in particular in RIKEN, where numerous experiments have been performed recently to test mass models and theoretical predictions of the drip lines. Different production mechanisms have been employed to these ends, for example, in-flight fission of a 345A MeV  $^{238}\text{U}$  and reactions with a  $^{48}\text{Ca}$  beam [10–12] to synthesise neutron-rich isotopes, and projectile fragmentation of a 345A MeV  $^{124}\text{Xe}$  beam [13] to produce nuclei at the proton drip line.

In the present experiment, a wide range of  $N \sim Z$  nuclei in the vicinity of  $^{100}\text{Sn}$  was produced by fragmentation of a 345A MeV  $^{124}\text{Xe}^{52+}$  beam impinging on a 4 mm Be target. An average beam intensity of 30 pA was used during the 203 h of data taking. The isotopic separation of fragments was achieved using two 2.85 and 2.17 mm thick aluminum achromatic energy degraders positioned at the  $F1$  and  $F5$  momentum dispersive foci of the BigRIPS separator [9].

The nuclei were identified on an event-by-event basis through the  $B\rho - \Delta E - \text{TOF}$  method in which the atomic number  $Z$  and the mass-to-charge ratios  $A/Q$  are deduced from the measurements of time of flight (TOF), magnetic rigidity ( $B\rho$ ), and energy loss ( $\Delta E$ ). The selected fragments were stopped at the final focal plane of the zero degree spectrometer (ZDS) [14] in the wide-range active silicon strip stopper array for beta and ion detection (WAS3ABi). This detector consists of 3 highly segmented (60 strips horizontally and 40 strips vertically) 1 mm thick double-sided silicon strip detectors used for the implantation of heavy ions, and a stack of ten 1 mm thick single-sided silicon strip detectors used to measure the energy of  $\beta$  particles emitted in the decay of implanted nuclei. Each single-sided silicon strip detector is vertically segmented into 7 strips allowing “ $\beta$  tracking” and reconstruction of the total energy of the detected  $\beta$  particles. The  $\gamma$ -ray detector, EUroball Riken cluster array (EURICA) [15], consisting of 84 HPGe crystals was installed around WAS3ABi in order to detect  $\beta$ -delayed  $\gamma$  rays, as well as delayed  $\gamma$  rays emitted from the isomeric states of implanted nuclei. An array of 18  $\text{LaBr}_3(\text{Ce})$  [16,17] detectors was also installed for fast-timing measurements.

The particle identification was verified by detecting the characteristic  $\gamma$  rays of known isomeric states in  $^{98}\text{Cd}$  and  $^{96}\text{Pd}$ . Background events coming from reactions and scattering of secondary beam in different materials along the beam line are excluded by checking beam profiles and various correlation plots made of pulse-height and timing signals in the beam line detectors following procedures given in Refs. [18,19]. The resulting particle identification plot is shown in Fig. 1. The relative root mean square  $Z$  and  $A/Q$  resolutions for Sn and  $N = Z$  isotopes are 0.41% and 0.052%, respectively. Four new isotopes, namely,  $^{96}\text{In}$ ,  $^{94}\text{Cd}$ ,  $^{92}\text{Ag}$ , and  $^{90}\text{Pd}$ , have been clearly identified with 2, 3, 8, and 2 events, correspondingly. Simultaneously, 2049 events of  $^{100}\text{Sn}$  were observed corresponding to an average production rate of 10 events per hour. The number of  $^{100}\text{Sn}$  events identified in this experiment is about 10 times higher than that in all previous experiments together.

During the experiment more than 10 different BigRIPS configurations were used. In the following only 2 of them for which transmissions are identical within 10% were selected. From the smooth systematics of the number of produced nuclei along different  $T_z = (N - Z)/2$  isospin lines (except for the  $T_z = -1/2$ ), a significant drop in the number of observed counts of  $^{93}\text{Ag}$  (31 counts) and  $^{89}\text{Rh}$  (0 counts) with respect to the neighboring isotopes with the same  $T_z$  value has been observed (Fig. 2).

These observations show with a confidence level larger than  $10\sigma$  that  $^{93}\text{Ag}$  and  $^{89}\text{Rh}$  are new proton emitters with half-lives lower than or comparable to the time of flight 760 ns through the BigRIPS and ZDS. It was already hinted by Moschner *et al.* that  $^{93}\text{Ag}$  can undergo fast decay of the order of  $\mu\text{s}$ , or with a long decay of the order of 1 s [20]. For two-proton ground-state emission observed previously in  $^{45}\text{Fe}$ ,  $^{48}\text{Ni}$ , and  $^{54}\text{Zn}$  with a simple scaling, the production rates were close to those predicted by EPAX [21–23]. Therefore, the evolution of the rates in the present experiment was assumed to be the same for bound and unbound

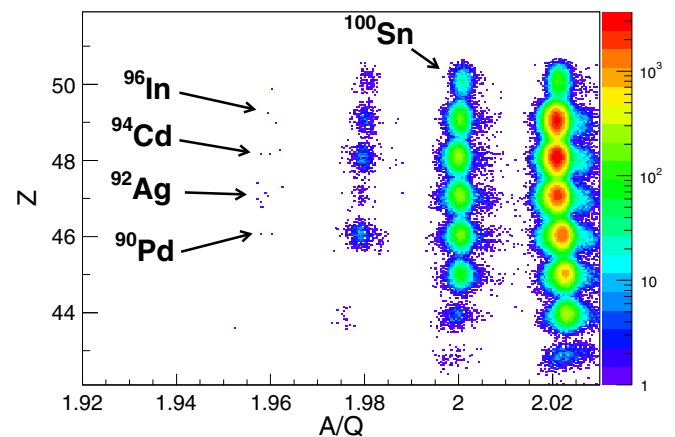


FIG. 1. The  $Z$  versus  $A/Q$  particle identification plot zoomed at most neutron-deficient isotopes produced in this experiment. The new isotopes are indicated.

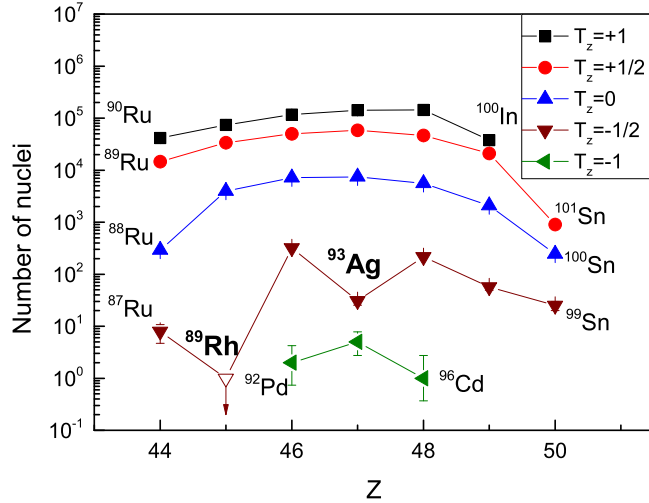


FIG. 2. Isotope production along different  $T_z$  lines. The open triangle corresponds to the upper limit (1 count) of the observation of  $^{89}\text{Rh}$ .

nuclei.  $^{93}\text{Ag}$  is the first case of observation of a one-proton ground-state emitter produced in fragmentation whose lifetime is comparable to the time of flight through the separator. The corresponding half-lives of proton emitters can be deduced more precisely from the measured time of flight using the assumption that the ratio between the number of identified nuclei with the same  $T_z$  value is the same as for the neighboring  $T_z$  line; i.e.,  $N(^{95}\text{Cd})/N(^{93}\text{Ag}) = N(^{96}\text{Cd})/N(^{94}\text{Ag})$ . The half-life of  $^{93}\text{Ag}$  is estimated to be  $T_{1/2} = 228 \pm 16$  ns. Since a smooth evolution of the number of produced nuclei shows that there is no cut in transmission, and since the ratio of transmissions of neighboring nuclei calculated by the LISE++ code [24] is practically constant, our method to estimate half-lives eliminates systematic errors.

Following the same procedure, assuming one count of  $^{89}\text{Rh}$  and systematics of neighboring nuclei, an upper limit of the half-life of  $^{89}\text{Rh}$  is deduced to be 120 ns.

One should mention that the proton emission can occur in  $^{93}\text{Ag}$  and  $^{89}\text{Rh}$  from the ground state or/and from an isomeric excited state. In the following we assume the ground-state proton emission only.

In the insets of figures Figs. 3(a) and 3(b), the deduced half-lives of  $^{93}\text{Ag}$  and  $^{89}\text{Rh}$  are compared with predictions of a simple model of proton emission [25] using  $S_p$  values calculated by various mass models: the finite-range droplet model (FRDM) [26], the Koura-Tachibana-Masahiro-Ueno-Yamada (KTUY05) model [27], the atomic mass evaluation (AME2012) [28], the Duflo-Zuker model [29], and the Hartree-Fock-Bogoliubov (HFB27) [30] model.

The separation energies were calculated assuming that the proton is emitted from the  $\pi g_{9/2}$  level, i.e., from an orbital with an  $l = 4$  angular momentum. Taking into account uncertainty on the parameters of the model [25],

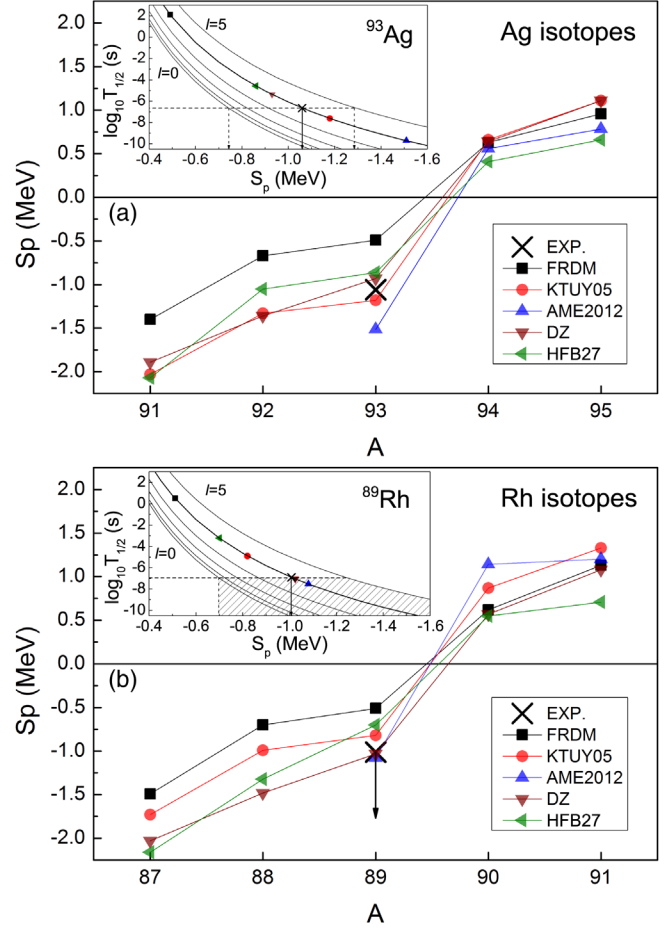


FIG. 3. Proton separation energy  $S_p$  for (a) Ag isotopes and (b) Rh isotopes according to different mass models: FRDM [26], KTUY05 [27], AME2012 [28], DZ28 [29], and HFB27 [30]. Deduced  $S_p$  for  $^{93}\text{Ag}$  and its upper limit for  $^{89}\text{Rh}$  are indicated. Insets show  $T_{1/2}$  as a function of  $S_p$  for different angular momenta of emitted proton (from  $l = 0$  to  $l = 5$ ) for  $^{93}\text{Ag}$  and  $^{89}\text{Rh}$ . The angular momentum of emitted proton is assumed to be  $l = 4$  ( $g_{9/2}$  proton). The dashed area corresponds to possible half-lives and separation energies for  $^{89}\text{Rh}$ .

the proton separation energies, extracted from the  $^{93}\text{Ag}$  and  $^{89}\text{Rh}$  measured half-lives, are found to be  $S_p = -1060 \pm 30$  keV and  $S_p < -1000$  keV, respectively.

Comparing to neighboring nuclei, no drop in the number of detected  $^{97}\text{In}$  nuclei is observed. The half-life of  $^{97}\text{In}$  should therefore be considerably longer than the time of flight through the fragment separator. The lower limit of the half-life is estimated under the assumption that the number of  $^{97}\text{In}$  events is at least  $2\sigma$  lower than the observed number of counts. Thus, the estimated lower limit of the half-life of  $^{97}\text{In}$  is 3  $\mu\text{s}$ , which is compatible with a half-life of  $26_{-10}^{+47}$  ms deduced from a single event in the GSI experiment [31] and mixed Fermi plus Gamow-Teller mirror transition [32].

Combining the results obtained by Suzuki *et al.* [13], where the upper limits of the half-lives of  $^{81}\text{Nb}$  and  $^{85}\text{Tc}$  are

derived to be 38 and 42 ns, respectively, and half-lives or their limits for  $^{89}\text{Rh}$ ,  $^{93}\text{Ag}$ , and  $^{97}\text{In}$  reported in this work to be  $<120$  ns,  $228 \pm 16$  ns, and  $\geq 3 \mu\text{s}$ , respectively, we conclude that half-lives of  $N = Z - 1$  nuclei increase approaching  $Z = 50$  between  $^{81}\text{Nb}$  and  $^{97}\text{In}$  by at least a factor of 70 or more. This result clearly shows a stabilizing effect of the  $Z = 50$  shell closure.

Proton separation energies  $S_p$  of nuclei around  $^{100}\text{Sn}$  estimated by different mass models for Ag and Rh are presented in Figs. 3(a) and 3(b), respectively. All mass models predict that the nuclei  $^{97,96}\text{In}$ ,  $^{93,92}\text{Ag}$ , and  $^{89}\text{Rh}$  identified in this experiment should be unbound. At the same time all mass models, as well as a detailed analysis of the landscape of two-proton radioactivity by Olsen *et al.* [33], suggest that the newly identified ( $^{93}\text{Ag}$  and  $^{89}\text{Rh}$ ) and assumed ( $^{97}\text{In}$ ) proton emitters are stable against two-proton and alpha emission in the ground state.

The observation of the proton emitters  $^{93}\text{Ag}$  and  $^{89}\text{Rh}$  together with the mass model predictions clearly indicate that the proton drip line was crossed experimentally for  $Z = 47$  and 45.

The production and study of drip-line nuclei using projectile fragmentation require reliable predictions for the corresponding cross sections and a simulation of fragment separators. In order to deduce the production cross sections from the measured isotopic yields, it is necessary to determine the transmission efficiency to the final focal plane. The transmission was calculated using the Monte Carlo method available in the LISE++ code [24]. The production cross sections, presented in Table I, are deduced for nuclei with transmission larger than 5%. A systematic uncertainty, estimated to be  $\sim 50\%$ , originates from the determination of the beam intensity and transmission. The cross sections were not corrected for possible proton emitters except for the half-life of  $^{93}\text{Ag}$ , which we were able to deduce. The effect of the secondary reactions in the target was taken into account in order to deduce the production cross section. This effect was estimated using the empirical and energy invariant cross section formula

TABLE I. Transmission and measured production cross section corrected for the contributions of secondary reactions in the target using the EPAX3.01 [34] parametrization. Only statistical errors are indicated considering uncertainties for small numbers [35].

Isotope	Transmission (%)	Cross section (b)
$^{100}\text{Sn}$	26	$(7.5 \pm 0.5) \times 10^{-13}$
$^{99}\text{Sn}$	48.7	$(4.2 \pm 0.8) \times 10^{-14}$
$^{98}\text{In}$	11.5	$(13.7 \pm 0.3) \times 10^{-12}$
$^{97}\text{In}$	33.5	$(1.3 \pm 0.2) \times 10^{-13}$
$^{95}\text{Cd}$	17.1	$(1.0 \pm 0.1) \times 10^{-12}$
$^{94}\text{Cd}$	32.9	$(2_{-1}^{+3}) \times 10^{-14}$
$^{93}\text{Ag}$	6.6	$(3.3 \pm 0.2) \times 10^{-12}$
$^{92}\text{Ag}$	12.9	$(3_{-1}^{+2}) \times 10^{-14}$

EPAX3.01 [34] incorporated in the LISE++ code [24]. It was found that secondary reactions in the 4 mm Be target increase the production yields in the range between 11% and 35% for the nuclei indicated in Table I.

In Fig. 4, the production cross sections deduced from the present work are compared with the empirical cross section formulas EPAX2.15 [36] and EPAX3.01 [34], as well as previous measurements. These include a 1-day experiment to optimize the BigRIPS separator for the production and selection of  $^{100}\text{Sn}$  (labeled TEST) [37], an experiment performed at GSI in which the fragments from reactions of a 1A GeV  $^{124}\text{Xe}$  beam on a  $4 \text{ g cm}^{-2}$  Be target [8,38] were separated using the FRS separator (labeled ‘‘Straub’’), and the already mentioned experiment performed in RIKEN by Suzuki *et al.* [13].

One can notice a reasonable overall matching between the calculated and measured cross sections. A very good agreement is observed between the cross sections measured in the three different RIKEN experiments performed with the same beam-target combinations. In particular, the measured  $^{100}\text{Sn}$  cross section of  $(7.5 \pm 0.5 \pm 3.8_{\text{sys}}) \times 10^{-10}$  mb is in agreement within uncertainties with the value of  $(7.4 \pm 1.7 \pm 3.7_{\text{sys}}) \times 10^{-10}$  mb measured by Suzuki *et al.* [13]. The other interesting feature is the systematically larger cross sections observed in the GSI experiment [8,38] as compared to the RIKEN ones, suggesting a possible energy and/or target thickness dependence on the observed final yields.

Such a dependence can originate from the additional production yields via secondary reactions in the much thicker target used at GSI energies. The measured  $^{100}\text{Sn}$  production cross sections and production cross sections

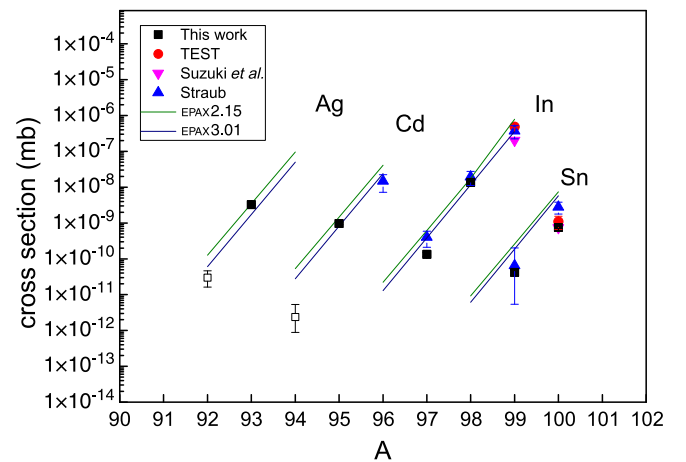


FIG. 4. Measured production cross sections from this work compared with experiments performed at the same energy, the TEST experiment [37], and Suzuki *et al.* [13], and at a higher beam energy [8,38]. The predictions of the empirical cross section formulas EPAX2.15 [36] and EPAX3.01 are indicated as well. The cross sections of new isotopes are indicated with open squares.

TABLE II. The measured  $^{100}\text{Sn}$  production cross sections and corrected for the effect of secondary reactions in the target using the EPAX3.01 formula. The two uncertainties represent statistical and systematic uncertainties, respectively.

Experiment (Be target thick.)	Cross section ( $\times 10^{-10}$ mb)	
	Measured	Corrected
This work (4 mm)	$8.7 \pm 0.6 \pm 4.4$	$7.5 \pm 0.5 \pm 3.8$
TEST [37] (8 mm)	$15.0 \pm 6.0 \pm 4.5$	$11.1 \pm 4.4 \pm 3.3$
Suzuki <i>et al.</i> [13] (4 mm)	$8.6 \pm 2.0 \pm 4.3^a$	$7.4 \pm 1.7 \pm 3.7$
Straub [38] (21.6 mm)	$58 \pm 21$	$28 \pm 10$

<sup>a</sup>Estimated from cross sections given in Ref. [13].

corrected for the effect of secondary reactions for different experiments are presented in Table II.

The total probability to produce the fragment of interest taking into account primary and secondary reactions is increasing with target thickness. For a  $4 \text{ g cm}^{-2}$  (21.6 mm) thick Be target and according to the EPAX3.01 parametrization, the gain is a factor 2.07. Correcting the GSI result for  $^{100}\text{Sn}$  [8] by this factor to obtain a “secondary reaction independent” cross section leads to a value of  $(2.8 \pm 1.0) \times 10^{-9}$  mb, which is in much better agreement with the cross sections measured at RIKEN.

We applied the same correction to data from the fragmentation of a 345A MeV  $^{124}\text{Xe}$  beam on a 8 mm Be target [37]. In this case, because of the lower target thickness, the correction factor is smaller and the adjusted production cross section for  $^{100}\text{Sn}$  is reduced by  $\sim 35\%$  to  $(11.1 \pm 4.4 \pm 5.5_{\text{syst}}) \times 10^{-10}$  mb. Again, this value is in better agreement with the cross sections measured using different target thicknesses.

In conclusion, several new isotopes,  $^{96}\text{In}$ ,  $^{94}\text{Cd}$ ,  $^{92}\text{Ag}$ , and  $^{90}\text{Pd}$ , have been unambiguously identified at the Nishina Center Radioactive Isotope Beam Factory in the fragmentation of a 345A MeV  $^{124}\text{Xe}$  beam on a Be target. With the newly identified even- $Z$  isotopes, we closely approach the drip line, while we identified odd- $Z$  isotopes beyond the proton drip line. We have demonstrated that  $^{93}\text{Ag}$  and  $^{89}\text{Rh}$  are new proton emitters in the submicro-second range. The corresponding one-proton separation energies were estimated using a simple model of proton emission. The data analysis also allowed us to estimate a lower limit of the half-life of  $^{97}\text{In}$ . Systematics of the half-lives of  $N = Z - 1$  nuclei in the vicinity of  $^{100}\text{Sn}$  clearly show the stabilizing effect of the  $Z = 50$  shell closure. The measured production cross sections, corrected for the contributions of secondary reactions, are in fair agreement for different experiments, but still a clarifying experiment is required to further resolve the alleged discrepancy between cross sections measured for  $^{100}\text{Sn}$  in experiments with different target thicknesses and energies.

The authors acknowledge the highly professional support of the managerial and operation staff of the RIKEN

Nishina Center. We acknowledge the EUROBALL Owners Committee for the loan of germanium detectors and the PreSpec Collaboration for the readout electronics of the cluster detectors. The authors acknowledge the support of the DFG cluster of excellence “Origin and Structure of the Universe.” Part of the WAS3ABi setup was supported by the Rare Isotope Science Project which is funded by the Ministry of Education, Science and Technology (MEST) and National Research Foundation (NRF) of Korea–KAKENHI(25247045). Part of this work was supported by the Natural Sciences and Engineering Research Council (NSERC) of Canada. This work was supported by LIA FJ-NSP France-Japan project. I. Č. would like to acknowledge the partial support of MESTD of Serbia under Project No. 171018. A. J. acknowledges support from the Spanish Ministerio de Economía y Competitividad via the project FPA2014-57196-C5-4-P. The authors thank Hubert Grawe for valuable discussions.

\*Corresponding author.  
icelikovic@vinca.rs

- [1] J. Erler, N. Birge, M. Kortelainen, W. Nazarewicz, E. Olsen, A. M. Perhac, and M. Stoitsov, *Nature (London)* **486**, 509 (2012).
- [2] J. Cerny, J. Esterl, R. A. Gough, and R. G. Sextro, *Phys. Lett.* **33B**, 284 (1970).
- [3] S. Hofmann, W. Reisdorf, G. Münzenberg, F. P. Heßberger, J. R. H. Schneider, and P. Armbruster, *Z. Phys. A* **305**, 111 (1982).
- [4] O. Klepper, T. Batsch, S. Hofmann, R. Kirchner, W. Kurcewicz, W. Reisdorf, E. Roeckl, D. Schardt, and G. Nyman, *Z. Phys. A* **305**, 125 (1982).
- [5] B. Blank and M. Borge, *Prog. Part. Nucl. Phys.* **60**, 403 (2008).
- [6] M. Pfützner, M. Karny, L. Grigorenko, and K. Riisager, *Rev. Mod. Phys.* **84**, 567 (2012).
- [7] R. K. Wallace and S. E. Woosley, *Astrophys. J. Suppl. Ser.* **45**, 389 (1981).
- [8] C. Hinke *et al.*, *Nature (London)* **486**, 341 (2012).
- [9] T. Kubo, *Nucl. Instrum. Methods Phys. Res., Sect. B* **204**, 97 (2003).
- [10] T. Ohnishi *et al.*, *J. Phys. Soc. Jpn.* **77**, 083201 (2008).
- [11] T. Ohnishi *et al.*, *J. Phys. Soc. Jpn.* **79**, 073201 (2010).
- [12] Z. Y. Xu *et al.*, *Phys. Rev. Lett.* **113**, 032505 (2014).
- [13] H. Suzuki *et al.*, *Nucl. Instrum. Methods Phys. Res., Sect. B* **317**, 756 (2013).
- [14] T. Kubo *et al.*, *Prog. Theor. Exp. Phys.* **2012**, 3C003 (2012).
- [15] P.-A. Söderström *et al.*, *Nucl. Instrum. Methods Phys. Res., Sect. B* **317**, 649 (2013).
- [16] Z. Patel *et al.*, *RIKEN Accel. Prog. Rep.* **47**, 13 (2014).
- [17] P. H. Regan *et al.*, *EPJ Web Conf.* **63**, 01008 (2013).
- [18] N. Fukuda, T. Kubo, T. Ohnishi, N. Inabe, H. Takeda, D. Kameda, and H. Suzuki, *Nucl. Instrum. Methods Phys. Res., Sect. B* **317**, 323 (2013).
- [19] D. S. Ahn *et al.*, to be published.
- [20] Moschner *et al.*, *EPJ Web Conf.* **93**, 01024 (2015).

- [21] B. Blank *et al.*, *Phys. Rev. Lett.* **94**, 232501 (2005).  
[22] B. Blank *et al.*, *Phys. Rev. Lett.* **84**, 1116 (2000).  
[23] B. Blank *et al.*, *Phys. Rev. Lett.* **77**, 2893 (1996).  
[24] O. B. Tarasov and D. Bazin, *Nucl. Instrum. Methods Phys. Res., Sect. B* **266**, 4657 (2008).  
[25] D. S. Delion, R. J. Liotta, and R. Wyss, *Phys. Rep.* **424**, 113 (2006).  
[26] P. Moller, J. R. Nix, and W. J. Swiatecki, *At. Data Nucl. Data Tables* **59**, 185 (1995).  
[27] H. Koura, T. Tachibana, M. Uno, and M. Yamada, *Prog. Theor. Phys.* **113**, 305 (2005).  
[28] M. Wang, G. Audi, A. H. Wapstra, F. G. Kondev, M. MacCormick, X. Xu, and B. Pfeiffer, *Chin. Phys. C* **36**, 1603 (2012).  
[29] J. Duflo and A. P. Zuker, *Phys. Rev. C* **52**, R23 (1995).  
[30] S. Goriely, N. Chamel, and J. M. Pearson, *Phys. Rev. C* **88**, 061302(R) (2013).  
[31] K. Straub *et al.*, GSI Scientific Report 2010, p. 151, 2011.  
[32] T. Faestermann, M. Gorska, and H. Grave, *Prog. Part. Nucl. Phys.* **69**, 85 (2013).  
[33] E. Olsen, M. Pfützner, N. Birge, M. Brown, W. Nazarewicz, and A. Perhac, *Phys. Rev. Lett.* **110**, 222501 (2013).  
[34] K. Sümmerner, *Phys. Rev. C* **86**, 014601 (2012).  
[35] G. J. Feldman and R. D. Cousins, *Phys. Rev. D* **57**, 3873 (1998).  
[36] K. Sümmerner and B. Blank, *Phys. Rev. C* **61**, 034607 (2000).  
[37] I. Čeliković, Ph.D. thesis, Université de Caen Basse-Normandie, 2013.  
[38] K. Straub, Ph.D. thesis, Technische Universität München, 2011.